Polymer Brushes Grafted from Clay Nanoparticles Adsorbed on a Planar Substrate by Free Radical Surface-Initiated Polymerization

Xiaowu Fan,[†] Chuanjun Xia,[†] Timothy Fulghum,[‡] Mi-Kyoung Park,[‡] Jason Locklin,[†] and Rigoberto C. Advincula*[,†,‡]

Department of Chemistry and Tri-campus Materials Science Program, University of Alabama at Birmingham, Birmingham, Alabama 35294-1240, and Department of Chemistry, University of Houston, Houston, Texas 77204

Received June 6, 2002. In Final Form: October 31, 2002

The investigation of polymer brushes grafted from layered clay nanoparticles adsorbed on flat surfaces is reported. The protocol involves adsorption of clay nanoparticle layers on self-assembled monolayer-modified flat surfaces of Si wafers (SiO_x) and Au-coated glass. Organic cation free radical initiators were then adsorbed electrostatically onto the nanoparticle layer providing functionality for free radical surface-initiated polymerization (SIP). In this manner, grafting of the polymer from clay nanoparticle surfaces was observed in situ as compared to SIP procedures using particle dispersion in solution or in bulk. Surface sensitive spectroscopic and microscopic analytical techniques were used to characterize these polymer brushes. A comparison is made on similar free radical SIP protocols where the polymer was grafted directly from flat SiO_x and Au surfaces. Important issues on initiator density, substrate effects, and initiator stability are discussed with respect to polymer brush molecular weight, conformation, and grafting density. The protocol provides a general procedure for preparing model substrate surfaces to investigate SIP mechanism on particle and nanoparticle surfaces.

Introduction

Grafting polymer brushes onto solid surfaces has attracted intensive interest in recent years because of potential applications in colloidal stabilization,[1] lithography,[2] biocompatibility,[3] electronic devices,[4] and nanocomposite materials.[5] As compared to chemisorption and physisorption of preformed polymers,[6,7] much attention is being focused on densely grafted polymer brushes through surface-initiated polymerization (SIP), in which chain growth is promoted from initiators already attached to the surface.[8] This is mainly because in the former approach, initially grafted chains (at the beginning of adsorption) sterically shield remaining active sites on surfaces, resulting in limited graft density and thickness of polymer brushes.[9] The advantage of SIP is that high-density polymer brushes are accessible where the average distance between grafting points is much smaller than the radius of gyration (R_g). A wide variety of polymerization methods have been applied toward SIP protocols on surfaces including free radical polymerization,[10,11] anionic polymerization,[12,13] atomic transfer radical polymerization (ATRP),[14] and polymerizations by 2,2,6,6-tetramethyl-1-piperidyloxy (TEMPO).[15]

The preparation of clay nanocomposite materials is also of great interest toward basic materials properties and applications, i.e., improved mechanical, thermal, and barrier properties of polymer composites.[16] Clay nanoparticle platelets, e.g., montmorillonite aluminosilicates, have a distinctive two-dimensional topology, i.e., the thickness of clay nanoparticles is ca. 1 nm while lateral dimensions are in hundreds of nanometers. They are derived from exfoliation of layered aluminosilicate clays and have been widely incorporated as inorganic species in polymer-layered silicate (PLS) nanocomposite materials[17] and ultrathin films.[18] A unique property of layered clays is the presence of exchangeable metal cations such as Na^+, Li^+, and Ca^{2+}, etc. at the spacing between negatively charged aluminosilicate layers. As a result, positively charged organic cations can be attached onto

* To whom correspondence should be addressed.
[†] University of Alabama at Birmingham.
[‡] University of Houston.

(1) Halperin, A.; Tirrell, M.; Lodge, T. P. *Adv. Polym. Sci.* **1992**, *100*, 31.
(2) Prucker, O.; Schimmel, M.; Tovar, G.; Knoll, W.; Ruhe, J. *Adv. Mater.* **1998**, *10*, 1073.
(3) Ratner, B. *J. Biomed. Mater. Res.* **1993**, *27*, 837.
(4) Bawden, M. J.; Turner, S. R. In *Electronic and Photonic Applications of Polymers*; Advances in Chemistry Series, 218; American Chemical Society: Washington, DC, 1988.
(5) Giannelis, E. P.; Krishnamoorti, R.; Manias, E. *Adv. Polym. Sci.* **1999**, *138*, 107.
(6) Fleer, G. J.; Cohen-Stuart, M. A.; Scheutjens, J. M. H. M.; Cosgrove, T.; Vincent, B. *Polymers at Interfaces*; Chapman & Hall: London, 1993.
(7) Koberstein, J.; Laub, C. *Polym. Prepr. Am. Chem. Soc., Div. Polym. Chem.* **1999**, *40*, 126.
(8) Zhao, B.; Brittain, W. J. *Prog. Polym. Sci.* **2000**, *25*, 677.
(9) Balazs, A.; Lyatskaya, Y. *Macromolecules* **1998**, *31*, 6676.
(10) (a) Prucker, O.; Ruhe, J. *Macromolecules* **1998**, *31*, 592. (b) Prucker, O.; Ruhe, J. *Macromolecules* **1998**, *31*, 602. (c) Biesalski, M.; Ruhe, J. *Macromolecules* **1999**, *32*, 2309.
(11) Huang, W.; Skanth, G.; Baker, G. L.; Bruening, M. L. *Langmuir* **2001**, *17*, 1731.
(12) (a) Zhou, Q.; Wang, S.; Fan, X.; Advincula, R.; Mays, J. *Langmuir* **2002**, *18*, 3324. (b) Zhou, Q.; Fan, X.; Xia, C.; Mays, J.; Advincula, R. *Chem. Mater.* **2001**, *13*, 2465.
(13) (a) Jordan, R.; Ulman, A.; Kang, J.; Rafailovich, M.; Sokolov, J. *J. Am. Chem. Soc.* **1999**, *121*, 1016. (b) Quirk, R.; Mathers, R. *Polym. Bull.* **2001**, *6*, 471.
(14) (a) Ejaz, M.; Yamamoto, S.; Ohno, K.; Tsujii, Y.; Fukuda, T. *Macromolecules* **1998**, *31*, 5934. (b) Huang, W.; Kim, J.-B.; Bruening, M. L.; Baker, G. L. *Macromolecules* **2002**, *35*, 1175. (c) Kim, J.-B.; Bruening, M. L.; Baker, G. L. *J. Am. Chem. Soc.* **2000**, *122*, 7616.
(15) Husseman, M.; Malmstrom, E. E.; McNamara, M.; Mate, M.; Mecerreyes, D.; Genoit, D. G.; Hedrick, J. L.; Mansky, P.; Huang, E.; Russell, T. P.; Hawker, C. J. *Macromolecules* **1999**, *32*, 1424.
(16) Krishnamoorti, R.; Vaia, R. *Polymer Nanocomposites*; ACS Symposium Series 804; Oxford University Press: North Carolina, 2002.
(17) Alexandre, M.; Dubois, P. *Mater. Sci. Eng.* **2000**, *28*, 1.
(18) Kleinfeld, E. R.; Ferguson, G. S. *Science* **1994**, 265, 370.

10.1021/la026039u CCC: $25.00
Published on Web 12/28/2002

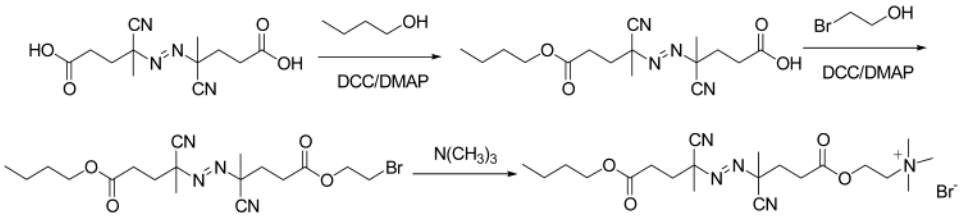

Figure 1. Synthetic scheme and structure of the cationic free radical initiator.

clay interfaces electrostatically by cation exchange processes. In principle, organic SIP initiators with a cationic group can be attached to clay surfaces by ion exchange procedures. Polymer−clay nanocomposites prepared from SIP reactions directly on clay particles have the advantage of increased dimensional stability and superior properties as compared to physical blends.[16,17]

There have been efforts in the past to do SIP from clay surfaces and layers via charged initiator attachment through living anionic SIP (LASIP)[19] and living free radical polymerization (LFRP) method.[20] A free radical SIP strategy was also applied to high surface area mica powder by attaching an azo initiator 2,2′-azobis(isobutyramidine hydrochloride) (AIBA) on the particles.[21] All of these strategies involved taking solution dispersions of bulk clays (exfoliated and unexfoliated) and "priming" the clay particles with SIP initiator. Polymer chains are grafted both at the surface and at the inner lamellae spacing of the clay particles. These methods have the advantage of obtaining a large sample of grafted polymers due to high surface/volume ratio of particles. The grafted polymers can then be desorbed and analyzed through conventional polymer characterization methods.[19] However, a disadvantage with this method is that it is not possible to investigate polymer brush formation in situ from the surface of clays and investigate effects of two-dimensional confinement in the polymerization mechanism. Theoretical investigations have shown that chain growth in a two-dimensional topology results in lower MW polymers with a higher polydispersity of polymer chain lengths.[22] This results from differences in diffusion properties of monomers and reactivity of propagating chain ends of different chain lengths. Also, with SIP on particles, it is not possible to distinguish effects of particle aggregation, solubility, and desorption of initiators from the polymerization mechanism at surfaces. With unexfoliated clay particles, this is also complicated by polymerization within the confined lamellar interfaces of the particle.

To observe directly the formation of polymer brushes on clay surfaces, we investigated an SIP protocol utilizing adsorbed clay nanoparticle platelets on flat surfaces. To the best of our knowledge, polymer brushes grafted from clay nanoparticle surfaces on a solid support substrate by free radical SIP have not been reported. The significance of this investigation and protocol is that other particles and nanoparticles can be similarly investigated, e.g., their adsorption on flat surfaces, to which polymer brushes can be grafted in situ using SIP. The advantage is that a variety of surface sensitive spectroscopic and microscopic techniques can be applied to characterize the polymer layers on flat substrate surfaces. It also provides a simplified

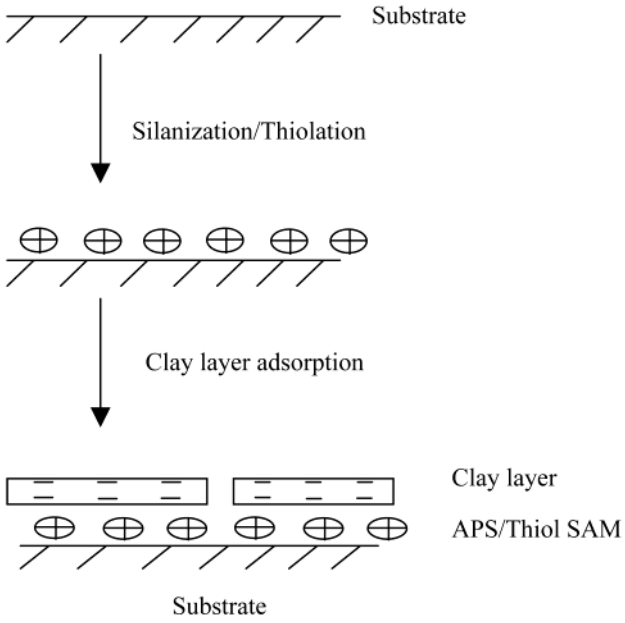

Figure 2. Surface modification by SAM and electrostatic nanoparticle clay layer adsorption.

model for studying SIP processes on surfaces as compared to procedures using particle dispersions. In contrast, most studies of SIP on flat surfaces have been done directly on polished silicon wafers (SiO_x),[24] glass,[23] and Au[11] substrates. The protocol can thus be applied to the investigation of differences between free radical, anionic, cationic, ATRP, and TEMPO polymerization mechanisms on dispersed particles and nanoparticle "layers" adsorbed on flat surfaces.

In this work, polystyrene brushes were grafted from adsorbed montmorillonite clay nanoparticles on both Si wafer and gold flat substrates. Both substrates were modified to have a positive charge using self-assembled monolayers (SAMs) of amphiphiles to which a layer of the negatively charged clay nanoparticle platelets was adsorbed. A cationic 2,2′-azobis(isobutyronitrile) (AIBN) type initiator with a quaternized amine end group was first synthesized (Figure 1) and then electrostatically adsorbed onto the clay layer (Figures 2 and 3). The substrate was then used for polymerization of styrene monomers by free radical SIP protocol (Figure 4). Similar SAMs of modified azo initiators with silane and thiol end groups have already been employed for free radical SIPs on flat silicon (SiO_x)[24] and gold surfaces.[11,25] Using a number of surface sensitive spectroscopic and microscopic techniques, we investigated differences between SIP using ionically attached initiators and that of covalently bound initiators in terms of graft density, polymer layer thickness, and roughness.[24] From

(19) Fan, X.; Zhou, Q.; Xia, C.; Cristofoli, W.; Mays, J.; Advincula, R. C. *Langmuir* **2002**, *18*, 4511.
(20) Weimer, M. W.; Chen, H.; Giannelis, E. P.; Sogah, D. Y. *J. Am. Chem. Soc.* **1999**, *121*, 1615.
(21) Meier, L.; Shelden, R.; Caseri, W.; Suter, U. *Macromolecules* **1994**, *27*, 1637.
(22) Wittmer, J.; Cates, M.; Jhoner, A.; Turner, M. *Europhys. Lett.* **1996**, *33*, 397.
(23) Minko, S.; Gafijchuk, G.; Sidorenko, A.; Voronov, S. *Macromolecules* **1999**, *32*, 4525.
(24) Prucker, O.; Ruhe, J. *Langmuir* **1998**, *14*, 6893.
(25) Schmidt, R.; Zhao, T.; Green, J.-B.; Dyer, J. D. *Langmuir* **2002**, *18*, 1281.

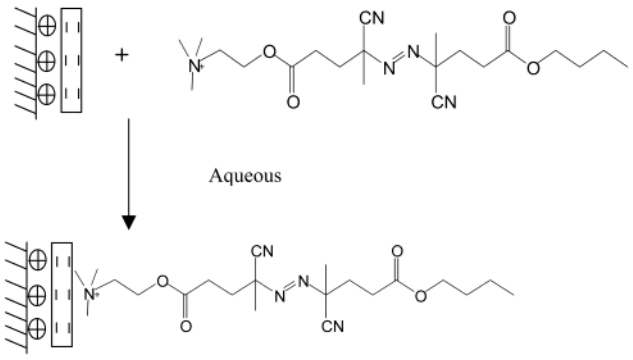

Figure 3. Schematics of initiator immobilization by cation exchange and electrostatic adsorption of organic cation initiator.

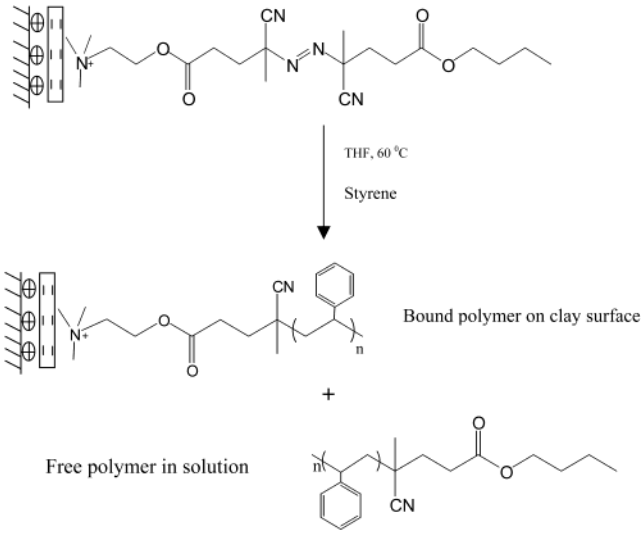

Figure 4. Schematics of grafting polymerization: bound and free polymers' chain growth.

molecular weight and polydispersity data, kinetics regarding chain growth in solution and thickness increase on surfaces was analyzed and discussed. The preliminary results in this work should be of theoretical and practical importance in investigating SIP mechanism on confined environments. For PLS nanocomposite synthesis, we are currently investigating intercalative free radical SIP procedures using the same initiators intercalated into galleries (lamellae) of dispersed clay nanoparticles.[26]

Experimental Section

Materials. Montmorillonite clay (commercially Cloisite Na^+, cation exchange capacity ~92 mequiv/100 g, surface area ~750 m^2/g) was provided by Southern Clay Products, Inc. Deionized water (resistivity = 18.2 MΩ, pH 6.82) used in all experiments was purified by a Milli-Q Academic system (Millipore Cooperation) with a 0.22 μm Millistack filter at the outlet. Styrene monomer (Aldrich) was distilled under reduced pressure at room temperature. All organic solvents used were purified by distillation before use. Reagents for initiator synthesis were purchased from Aldrich and used without further purification.

Boron-doped silicon wafers with surface orientation of ⟨100⟩ (MEMC Electronic Materials, Inc.) and gold-deposited (by thermal vacuum evaporation, ~48 nm in thickness) glass slides were cut into 1.0 × 2.6 cm^2 rectangular pieces. They were precleaned and SAM-modified using well-documented substrate cleaning and modification procedures.[27] After they were cleaned, the SiO_2 layer thickness was measured by ellipsometry to be about 1.9 nm and the gold layer thickness was confirmed by surface plasmon spectroscopy (SPS). 3-Aminoproyltriethoxylsilane (APS) was used to modify Si wafers and 2-(dimethylamino)-ethanethiol hydrochloride for the Au-coated glass.

Initiator Synthesis. *Butyl 4-{2-[4-(2-Bromoethoxy)-1-cyano-1-methyl-4-oxobutyl]diazenyl}-4-cyanopentanoate.* To a one neck flask was charged 11.2 g of 4,4′-azobis(4-cyanovaleric acid), 2.96 g of butanol, 0.06 g of 4-(dimethylamino)pyridine (DMAP), and 50 mL of dimethyl formamide (DMF). The homogeneous solution was cooled with an ice water bath before 8.26 g of 1,3-dicyclohexylcarbodiimide (DCC) was added in portions. The reaction mixture was allowed to react at 0 °C for 5 min and warmed to room temperature for 3 h. The urea was filtered, and the filtrate was poured into water, extracted with methylene chloride, washed by saturated sodium bicarbonate, and dried over magnesium sulfate. After the solvent was evaporated, the residue was solidified by pouring into cold hexanes. The solid (9.0 g) was collected, dried, and used for the next step without further purifications. ^{1}H NMR (in $CDCl_3$, δ in ppm): 4.11 (2H, t, 6.6 Hz), 2.47 (8H, m), 1.74 (3H, s), 1.68 (3H, s), 1.62 (2H, p, 7.1 Hz), 1.37 (2H, h, 7.3 Hz), 0.94 (3H, t, 7.3 Hz). ^{13}C NMR (in $CDCl_3$, δ in ppm): 174.82, 171.58, 117.59, 117.52, 71.96, 71.89, 65.05, 33.19, 31.66, 30.55, 29.21, 29.12, 23.98, 23.77, 19.11, 13.71. The crude product was reacted with 1 equiv of bromoethanol under the same DCC/DMAP conditions to give the title compound. The product was purified by crystallization from methanol. A 2.5 g amount of white solid was obtained (overall yield, 15%). The product was kept in a refrigerator in the dark. ^{1}H NMR (in $CDCl_3$, δ in ppm): 4.43 (2H, t, 6.2 Hz), 4.11 (2H, t, 6.6 Hz), 3.52 (2H, t, 6.1 Hz), 2.44 (8H, m), 1.74 (6H, s), 1.62 (2H, p, 7.1 Hz), 1.38 (2H, h, 7.6 Hz), 0.94 (3H, t, 7.4 Hz). ^{13}C NMR (in $CDCl_3$, δ in ppm): 171.37, 170.86, 117.43, 72.00, 71.82, 65.02, 64.31, 33.17, 33.07, 30.54, 29.09, 28.93, 28.47, 23.98, 19.10, 13.70.

2-({4-[2-(4-Butoxy-1-cyano-1-methyl-4-oxobutyl)diazenyl]-4-cyanopentanoyl}oxy)-N,N,N-trimethyl-1-ethanaminium Bromide. A 1.5 g amount of butyl 4-{2-[4-(2-bromoethoxy)-1-cyano-1-methyl-4-oxobutyl]diazenyl}-4-cyanopentanoate was stirred with excess of trimethylamine in anhydrous tetrahydrofuran (THF) for 2 days. The precipitate was collected and washed thoroughly with THF. After it was dried under vacuum, 1.4 g of the product was obtained (yield = 82%). ^{1}H NMR (in $CDCl_3$, δ in ppm): 4.62 (2H, h, 5.6 Hz), 4.20 (2H, t, 4.4 Hz), 4.10 (2H, t, 6.7 Hz), 3.53 (9H, s), 2.44 (8H, m), 1.76 (3H, s), 1.73 (3H, s), 1.62 (2H, p, 7.9 Hz), 1.38 (2H, h, 7.6 Hz), 0.94 (3H, t, 7.4 Hz). ^{13}C NMR (in $CDCl_3$, δ in ppm): 171.37, 170.75, 117.73, 117.68, 72.19, 71.71, 65.06, 64.75, 58.45, 54.35, 33.05, 30.53, 29.09, 23.81, 23.78, 19.10, 13.71.

Preparation of Flat Clay Surfaces. A 0.01 wt % aqueous montmorillonite Na^+ dispersion was prepared for clay layer deposition. The yellowish dispersion was stirred with a blender at 2000 rpm overnight. After the dispersion was sonicated for half an hour, both modified Si wafer and gold substrates were submerged into the clay dispersion for 15 min, followed by rinsing with deionized water and drying with airflow.

Initiator Immobilization. The cationic AIBN derivative can be attached to clay surfaces by electrostatic attraction (physisorption). The initiator was first dissolved in deionized water to make a 1.25 wt % aqueous solution. Substrates with adsorbed clay nanoparticles as the top layer were soaked in the initiator solution overnight at room temperature and then cleaned by extensive rinsing with deionized water and drying with continuous air flow. All substrates were kept in a desiccator prior to SIP.

(26) (a) Fan, X.; Xia, C.; Advincula, R. *Colloids Surf. A*, submitted for publication. (b) Fan, X.; Xia, C.; Advincula, R. Manuscript in preparation.

(27) The substrates were soaked in Piranha solution (3:7 (v/v) mixture of 30% (w/w) hydrogen peroxide and 98% (w/w) sulfuric acid, 15 min for silicon wafer and 1 min for gold substrates) and thoroughly rinsed by sonication in a deionized water bath. The purpose for the above process was to create a fresh and clean surface suitable for the next step of SAM formation. The precleaned silicon wafer pieces were submerged into freshly distilled toluene along with 0.5 wt % of APS (Aldrich) for 30 min. The substrates were then sonicated with toluene, acetone, and deionized water and stored in 0.1 M HCl overnight for protonation. Gold surfaces were modified by dipping them into 5 mM solution of 2-(dimethylamino)ethanethiol hydrochloride (Aldrich) in ethanol for 1 h, followed by thorough rinsing by ethanol. The purpose of the above pretreatment process was to generate a positively charged SAM of silane or thiol for the subsequent clay layer adsorption. Water contact angle measurements were taken before and after SAM to ensure surface functionalization by monitoring the change in hydrophilicity of the substrates.

Grafting Polymer Layers from Clay Surfaces. Initiator-modified clay nanoparticle layers on silica and gold substrates were submerged to a solution of 5 mL of THF and 10 mL of styrene in a reaction flask for Schlenck procedures. The system was purged for 1 h under nitrogen flow. Afterward, the flask was immersed on a silicon oil bath and the temperature was increased to 60 °C. The reaction was maintained under nitrogen atmosphere for 4 and 8 h. For each of the two reactions, four substrates were used for polymerization. After polymerization, the substrates were removed from solution and reaction flask. The solution, which contained free polymer, was decanted and the polymer was isolated for molecular weight analysis (precipitated in methanol). Before surface analysis, all substrates were washed for 24 h in toluene using a Soxhlet extraction apparatus to remove any unbound polymers from the clay surfaces (physisorbed vs grafted). The substrates were then vacuum oven-dried prior to surface analysis.

Characterization and Instrumentation. *IR Spectroscopy.* The transmission Fourier transform (FT)-IR spectra of the polystyrene-grafted samples was obtained on a Nicolet NEXUS 470 FT-IR system. The silicon wafer with polystyrene layers on both sides was scanned 512 times with a resolution of 4 cm^{-1}.

X-ray Photoelectron Spectroscopy (XPS). All samples were analyzed using a Kratos Axis 165 Multitechnique Electron Spectrometer system. A nonmonochromatic Al Kα X-ray source (1486.6 eV) operated at 15 kV and 20 mA was applied to excite the photoelectron emission. Fixed analyzer transmission (FAT) mode was used, and survey scans (spot 800 × 200 um^2, resolution 4 eV at analyzer pass energy of 160 eV) were collected from 0 to 1400 eV to obtain elemental composition of the samples. The C 1s peak of hydrocarbon signal (284.5 eV) was used as the binding energy reference. A built-in charge neutralizer was operated to compensate for charge build-up during the measurements.

Atomic Force Microscopy (AFM). The surface morphologies of planar samples were studied using a PicoScan system (Molecular Imaging) equipped with a 7 × 7 μm^2 scanner. Magnetic AC (MAC) mode was used for all of the AFM images. The MAC lever, silicon nitride-based cantilever coated with magnetic film, was used as the AFM tip. The force constant of the tip was 0.5 N/m, and the resonance frequency was around 100 kHz. To study the morphology of pristine clay particles, a drop of clay dispersion was spread onto a piece of modified Si wafer. After the water was evaporated, the AFM micrograph was taken. All samples were measured inside a suspension chamber to minimize ambient temperature and vibration disturbance. The root mean square (RMS) surface roughness was calculated using integrated software for image analysis.

SPS. For the gold-coated substrates, the surface plasmon resonance spectra were recorded on a Multiskop system (Optrel GmbH, Germany). Using the Kretschmann configuration and attenuated total reflection (ATR) conditions,[28] the reflectance was monitored with a p-polarized He−Ne laser as a function of incidence angle. The thin film thickness data were obtained by fitting the surface plasmon resonance curves with a Fresnel equation algorithm using modeling software integrated with the Multiskop system (Winspall, version 2.0).

Ellipsometry. Using a 632.8 nm He−Ne laser beam as the light source, ellipsometric thickness measurements (60° incidence angle) were also performed (Mulitskop ellipsometer) for samples with silicon wafer as the substrate. Both δ and ψ values were measured, and the thickness data were calculated with the integrated modeling software module (Multi, Optrel, GbR.).

Contact Angle. Static contact angle measurements were made with water using a Tantec contact angle meter (model CAM Micro) on a horizontal stage. Measurements were within ±2° precision.

Gel Permeation Chromatography (GPC). Using polystyrene calibration standards (20 000−200 000 g/mol), GPC was used to determine the molecular weights and polydispersity indices of free polystyrene formed in solution.

Results and Discussion

The substrate preparation and SIP process are illustrated in the schematic diagrams of Figures 2−4. The substrates were analyzed using surface sensitive spectroscopic and microscopic techniques after each surface modification process. First of all, it is important to verify the integrity of adsorbed clay and initiator layers. The chemical species present (XPS and IR), thickness data (ellipsometry and SPS), and morphology (AFM) of the substrates before polymerization indicate the success of clay nanoparticle and initiator layer formation. The same analytical techniques were subsequently used to validate the formation of grafted polymer brushes on these substrates. In this manner, important features different from previously reported free radical SIP on flat and polished Si wafer and Au substrates were observed and will be discussed.

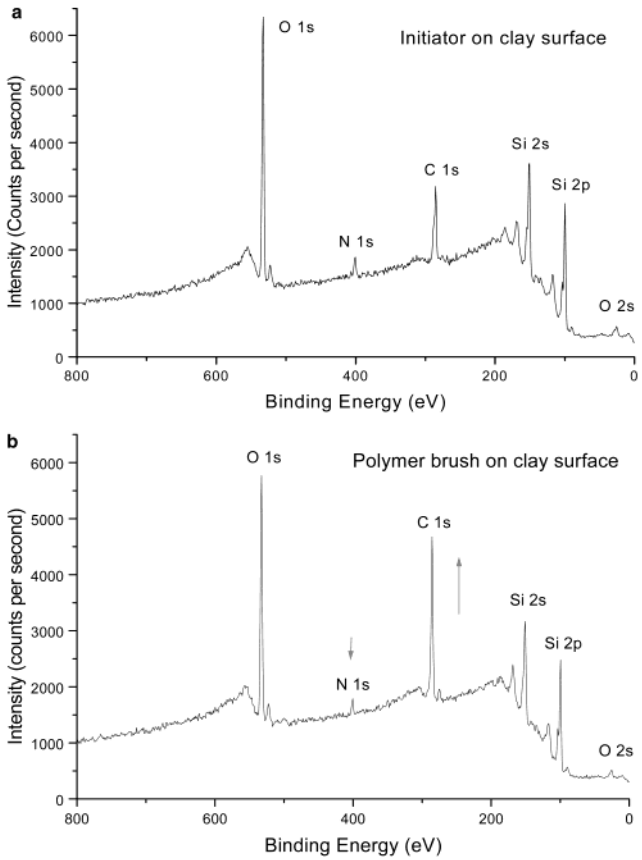

Figure 5. (a) XPS spectra of composite layers of APS, clay nanoparticles, and cationic free radical initiator adsorbed on Si wafer substrate. (b) XPS spectra of composite layers of APS, clay nanoparticles, and cationic free radical initiator adsorbed on Si wafer substrate and grafted polystyrene polymer.

XPS. To begin, XPS measurements were used to qualitatively verify the presence of the initiator attached to the surface and grafted polymer brushes from the modified clay surface. It should be pointed out that every polymer brush sample was thoroughly washed by Soxhlet extraction before surface analysis. The nonpolar toluene solvent was selected to preferentially extract polystyrene and prevent desorption of electrostatically adsorbed clay and grafted polymer. This procedure is necessary to remove all of the unbound polymer formed in solution during SIP.[24] Figure 5 a,b are survey scan spectra of silicon wafer samples after initiator immobilization and after 8 h of SIP, respectively. In Figure 5a, C 1s (286 eV) and N 1s (400 eV) peaks indicate the attachment of charged initiator molecules on the underlying clay layer. In Figure 5b, the increased C 1s and decreased N 1s signal intensities after polymerization demonstrate the presence of higher molecular weight polymer (polystyrene) layers grafted

(28) Knoll, W. *MRS Bull.* **1991**, *16*, 29.

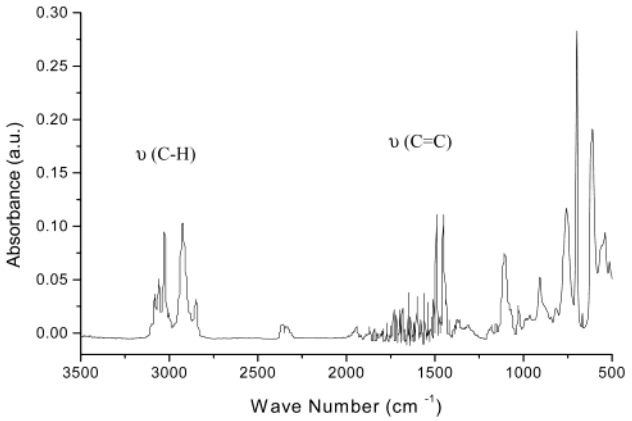

Figure 6. Transmission IR spectrum of a composite silicon wafer substrate with polystyrene brush layer.

Table 1. Summary of Thickness, Roughness, and Contact Angle Data of the Different Layers on Si Wafer Substrate

layer	thickness (nm)	roughness (RMS) by AFM (nm)	contact angle (water) (deg)
APS	1.0 ± 0.1		
clay	2.2 ± 0.2	3.2	40 ± 2
initiator	1.1 ± 0.2		65 ± 2
polystyrene (8 h SIP)	8.8 ± 0.5	4.1	81 ± 2

from the initiator layer. Furthermore, in the two spectra, peaks of O 1s, Si 2s, and Si 2p were also observed.[29] This can be attributed to exposure of silicate clay or silicon (SiO_x layers) underneath. Similar XPS results were obtained by Prucker and Ruhe.[24] However, the polymer layers grafted from flat SiO_x surface through a SAM of silane initiators could screen all signals from the underlying initiator and substrate, because the 40 nm thick polymer layer is higher than the escape depth of the photoelectron (about 10 nm). A comparison of results suggests that the polymer layer thickness grafted from clay surfaces is less than the escape depth of the photoelectron and/or the clay layer underneath is not uniformly covered by the polymer brush layer. This analysis is further substantiated by ellipsometry and AFM results.

Infrared Spectroscopy. Figure 6 shows the IR spectrum of a Si wafer sample after 8 h growth of the polystyrene brush layer. As labeled in the figure, the vibrational bands typical for polystyrene, such as C−H aromatic and aliphatic stretching at 3100−2800 cm^{-1} (2938 cm^{-1} for overlapping CH_3 and CH_2 bands, 2846 cm^{-1} for the CH_2 symmetric stretch) and C═C vibrations at 1490 and 1450 cm^{-1}, are clearly observed. This is consistent with previously reported FT-IR spectra of grafted polystyrene brushes.[11,24,25] Strong peaks below 1250 cm^{-1} are attributed to vibrations of the bonds in the metal oxides of montmorillonite clay and silica layer on Si wafer. It is not possible to distinguish the fine features of the spectra attributed to the polymer in this region. Nevertheless, the results verify the grafting of polymer brushes on the adsorbed clay nanoparticle layer.

Contact Angle Measurements. Table 1 summarizes the results of contact angle measurements on each stage of substrate and graft polymer preparation. The hydrophilic nature of the clay nanoparticle platelets is revealed by the 40° static contact angle measured (water). This changed to 65° after electrostatic adsorption of the organic cation AIBN type initiator. This value is comparable to that reported by Dyer et al.[25] and Brittain et al.[30] on SAMs of analogous AIBN−thiol (64°) and AIBN−silane (68°) functionalized initiators on Au and Si wafer substrates, respectively. It indicates that sufficient coverage of clay nanoparticles by the initiator is achieved although not conclusive for packing arrangement and density. After grafting polymerization of polystyrene, the angle changed to 81° (83° before Sohxlet extraction). This value is lower than that reported previously by Dyer et al.[25] and Brittain et al.[30] at 88 and 92°, respectively (the value for spin-coated pure polystyrene is 98°, typical for the hydrophobic nature of this polymer). Thus, the lower contact angle indicates incomplete surface coverage of the clay/initiator layer by the grafted polystyrene and is supported by a higher RMS roughness (Table 1 and AFM data).

Ellipsometry. Table 1 also gives a summary of the average layer-by-layer ellipsometric thickness data as measured on silicon wafer substrates (four samples). The thickness of the APS layer agrees well with our previous work of surface silanization under the same experimental conditions and parameters.[31] A similar procedure for clay layer electrostatic adsorption was reported in our previous work[32] and by others.[18,33] Clay layer thickness is consistent with the average thickness data (ca. 2.56 nm) of layers deposited by alternate polyelectrolyte deposition (APD) involving the same type of clay.[32,33] The refractive index of montmorillonite used for thickness calculation was $n = 1.57$ similar to what has been reported on previous ellipsometry and SPS measurements.[33] A single montmorillonite crystal platelet has a thickness of about 1 nm. The data measured indicate that on the average 2−3 clay sheets were deposited onto the positively charged APS layer. We assume that this multilayer adsorption process should provide sufficient clay surface coverage for subsequent initiator immobilization. AFM surface morphology studies (discussed later) further corroborated this assumption.

A refractive index of $n = 1.5$ for the initiator layer was used for thickness calculation.[24] The thickness of the cationic initiator layer was lower than that of a similar silane-terminated AIBN initiator (ca. 1.3 nm), which was covalently bonded to Si wafer as reported by Prucker and Ruhe,[24] despite the fact that our AIBN derivative initiator is longer with six more C−C bonds than their monochlorosilane counterpart. The lower thickness may result from lower graft density of the initiators on clay surfaces, driven by a weaker ionic interaction. In contrast, surface silanization is realized by the reaction between the surface −OH groups and the −Cl ends of the chlorosilane molecules forming covalent bonds. By using the physical properties of the montmorillonite clay (charge density of 92 mequiv/100 g and surface area of 750 m^2/g) and assuming every charged site on the clay sheet is occupied by an initiator molecule, the graft density was calculated to be 0.37 molecules/nm^2. In comparison, a much higher graft density of approximately 2.7 molecules/nm^2 of chlorosilane on silicon wafer was determined using quartz

(29) Small symmetrical peaks to the left of the primary Si 2s and Si 2p lines are shake-up satellite peaks formed by valence electrons reorganization sometimes observed with the spectrum of silicon wafers. The rest of the photoelectron lines and secondary structures agree very well with the chemical species present in the sample. Signals of Mg and Al (relatively very small stoichiometrically as compared to Si and O) in the monolayer of clay are too weak to be detected.

(30) Sedjo, R.; Mirous, B. B. K.; Brittain, W. *Macromolecules* **2000**, *33*, 1492.
(31) Locklin, J.; Youk, J. H.; Xia, C.; Park, M.-K.; Fan, X.; Advincula, R. C. *Langmuir* **2002**, *18*, 877.
(32) Fan, X.; Park, M.-K.; Xia, C.; Advincula, R. *J. Mater. Res.* **2002**, *17*, 1622.
(33) Kotov, N. A.; Haraszti, T.; Turi. L.; Zavala, G.; Geer, R. E.; Dekany, I.; Fendler, J. H. *J. Am. Chem. Soc.* **1997**, *119*, 6821.

crystal microbalance (QCM) and ellipsometry (thickness 1.7 nm).[12,34] It should be noted that ellipsometric thickness is measured as an average area of the laser spot (a few square millimeters) on the sample surface. Therefore, the low thickness of the initiator layer cannot be solely attributed to an average lower graft density but also in terms of domain and aggregation behavior of the adsorbed initiators.

The refractive index of the polystyrene layer ($n = 1.59$) was assumed to be the same in the bulk state[35] and again has been used by other groups.[24] After 8 h of polymerization, the polystyrene layer grew to an average thickness of about 8.8 nm. This thickness is lower than that of (ca. 35 nm) polystyrene layer grafted directly from the Si wafer (without clay layers) through a similar free radical SIP protocol and conditions.[24] A lower graft density of the initiator layer can also explain this result as observed by Bruening et al. on direct polymerization on Au surfaces.[11] In this case, the stability of the initiator layer is an important consideration. The density of the initiator (actual percent of active initiators) has a direct bearing on polymer brush conformation and thickness. It can be ascertained that polymer chains from higher graft densities exist in the form of "bristles" or "brushes" due to interchain steric repulsion rather than "mushrooms" in sparsely grafted chains, i.e., the chains have enough space to expand in the lateral directions. This occurs as the average distance between grafting points becomes much smaller than the R_g. Assuming that the chain lengths are the same, the layer thickness should be much smaller for "mushroom" morphology than in the case of "brushes".[36] Experiments can be made to estimate polymer molecular weight on the basis of thickness and grafting density[37] and force−distance profiles of stretched end-tethered polymers.[38] However, these are indirect methods and subject to much experimental error and overinterpretation.

SPS. SPS is a technique of high sensitivity for characterizing thickness and optical properties of ultrathin films.[39] In this case, it was used to monitor the stepwise adsorption of APS, clay nanoparticles, and initiator and grafting of polystyrene from gold-coated substrates. Figure 7 shows the surface plasmon resonance curves from the series of thin film procedures. The shape and position of the curve is a function of thickness, d, and the refractive index, n. All scans show a narrow dip in reflectivity at a certain angle, resulting from the plasmon surface polariton resonance. Furthermore, the resonance angles stepwisely shift to higher values, indicating a thickness increase caused by each individual layer deposited. The thickness of each layer is indicated in the figure. Both clay layer and initiator thickness values are in good agreement with ellipsometric thickness data. It is worth mentioning that the thickness of grafted polymer after 4 h of SIP is 8.8 nm (average of four samples, Figure 7), which is nearly identical to that of the polymer layer after 8 h of SIP (Table 1). It can be hypothesized that a saturation limit in polymer layer growth is reached with respect to polymerization time for this system (discussed further in the next section). This is in contrast to a linear growth in thickness with polymerization time (at this thickness regime) with previously reported free radical SIP protocols.[24,11] In addition, the broader shape and the higher reflectivity at the plasmon curve minimum of the polymer layer indicate rougher films as compared to the underlying clay layer. Broadening of the SPS curve occurs as a function of superposition of several SPS curves from multiple resonances. This inhomogeneity is consistent with the observed morphology of the polymer brush surface as verified by AFM surface roughness measurement.

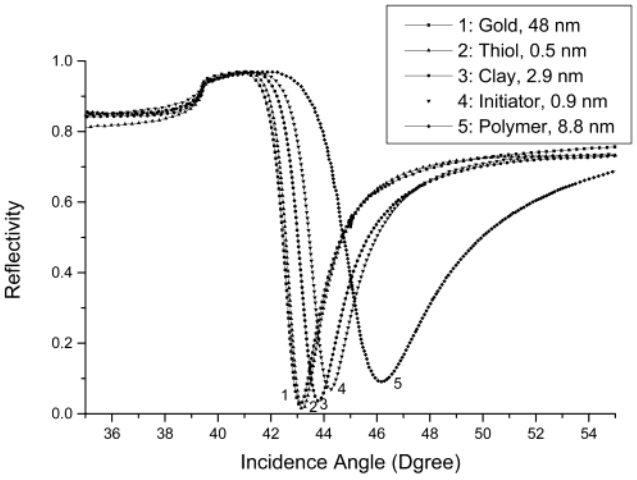

Figure 7. SPS spectra of composite layers of APS, clay nanoparticles, and cationic free radical initiator adsorbed on Si wafer substrate and grafted polystyrene polymer. Polymer layer was grafted by 4 h of SIP.

GPC. With the free radical SIP procedure, the immobilized AIBN initiator decomposes to form two free radicals. The bound radical gave rise to polymer brush grafted from clay surfaces; the other one to polymer chains grown freely in solution. GPC was used to analyze the free polymer products formed in solution. Figure 4 shows the presence of bound and free (unbound) polymers through free radical solution SIP as a consequence of the AIBN initiator design. Molecular weight of free polystyrene after 4 h of SIP was measured to be 86K with a polydispersity of 2.32 and 81K with a polydispersity of 2.49 as for 8 h of SIP. The two similar molecular weight and polydispersity indices are typical of ordinary free radical polymerizations, demonstrating that the reactions were indeed through a free radical mechanism. Considering the fast kinetics of free radical polymerizations, the similar molecular weights of the free polymers from the two polymerization times indicate that the reactions attained a steady state before or at 4 h, i.e., the chain length barely grew as the polymerization proceeded.

These data from free polymers in solution support the observed similar thickness values from ellipsometry and SPS for the two SIP grafting reaction times. It is reasonable to conclude that thickness growth reached a saturation state before or at 4 h of polymerization time. Again, this

(34) Zhou, Q.; Nakamura, Y.; Inaoka, S.; Park, M.; Wang, Y.; Mays, J.; Advincula, R. In *Polymer Nanocomposites*; ACS Symposium Series 804; Krishnamoorti, R., Vaia, R., Eds.; Oxford University Press: North Carolina, 2002.

(35) Brandrup, J.; Immergut, E. H. *Polymer Handbook*; J. Wiley & Sons: New York, 1989; V, 83.

(36) Luzinov, I.; Minko, S.; Senkovsky, V.; Voronov, A.; Hild, S.; Marti, O.; Wilke, W. *Macromolecules* **1998**, *31*, 3945.

(37) (a) From ref 13a, by swelling experiments, the molecular weight of a tethered polymer can be estimated. The height h of a brush in a good solvent is given by $h = (12/\pi)^{1/3} N \sigma^{1/3} (\omega/\nu)^{1/3}$, where ω is the excluded volume parameter, approximately (2 Å),[3] N is the number of monomers, and $\nu = (a^2/3)^{-1}$, with $a = 6.7$ Å (the Kuhn length for a polystyrene monomer unit). The polymerization degree can be expressed as $N = [1.074(h_{swollen})^{2/3}]/[h_{dry}(Å^2))^{1/2}]$. For example, when the thickness is 18 nm, the molecular weight calculated from the above equation is MW = 39 728 g/mol. (b) From ref 25, by accurate determination of thickness and surface density of dry films. Film thickness $= S_d(M_n/d)$, where M_n is the number average molecular weight, S_d is the surface density of the tethered polymer, and d is the density of the polymer (g/cm^3). Determination of M_n would be based on accurate determination of the film thickness and surface density of the tethered polymer.

(38) Al-Maawali, S.; Bemis, J.; Akhremitchev, B.; Leecharoen, R.; Janesko, B.; Walker, G. *J. Phys. Chem. B* **2001**, *105*, 3965.

(39) Knoll, W. *Annu. Rev. Phys. Chem.* **1998**, *49*, 569.

is in contrast to a linear thickness increase with time observed for polymer brushes grafted directly from a Si wafer surface, where "no saturation limit of the layer thickness is visible up to 12 h of polymerization"[24] and the initiator's half-life was measured to be 21 h at 60 °C via SIPs from silica gel nanoparticles.[10]

This difference in polymerization kinetics is clearly related to grafting densities of the initiator on the surface. It may also be related to the fact that bare clay surfaces are charged (more polar and ionic) as compared to a thick monolayer of the surface initiators (nonpolar). This could eventually contribute to slower and nonuniform monomer diffusion kinetics for SIP resulting in a more heterogeneous polymerization mechanism.[40,41] This point was recently emphasized to explain low molecular weight polymer brushes obtained by LASIP on Si wafers.[12] The effect of chain transfer reactions should also be investigated as there could be a dramatic difference between polymerization from the surface and what is found in solution. The effects of thiol-based initiators on chain transfer reactions with polymerizations in Au have been previously described by Bruening et al.[11] Because we observed similar thicknesses for grafting on clay-modified Au and SiO_x substrates, we believe that the present system was hardly affected by the Au−thiol initiator instability.[11] Another possibility is the desorption of the initiators from the surface during polymerization. Investigation of these differences and possible instabilities will contribute to a fundamental understanding of parameters affecting SIP mechanism at two-dimensionally confined surfaces. Further kinetics studies of this free radical SIP from flat and bulk clay surfaces are underway.

AFM. The morphology of pristine montmorillonite clay was first studied by AFM (Figure 8 a). The lateral dimension of adsorbed "nanoplatelets" is observed to be a few hundred nanometers and is consistent with previous observations employing the same exfoliation procedures.[32,33] Their thickness is between 1 and 3 nm (2.2 nm average) as determined by ellipsometry and SPS. The overlapping (amplitude flattened image) manner of clay sheet arrangements substantiates the thickness data. Therefore, the high aspect ratio characteristics of clay nanoparticles can be readily appreciated, forming flat "mosaic" layers on the substrate surface exposing large surface areas. The sharp edge profile of these sheets is also clearly seen. The morphology after adsorption of the initiator on the clay nanoparticle layers is shown in Figure 8b. As compared with Figure 8a, the organic cation initiators provide full coverage over the clay layers (sharp edges disappear), indicating strong electrostatic cohesion. This is necessary for subsequent initiator activation and polymerization in the SIP process. Full surface coverage was also observed in our previous work on alternating polyelectrolyte deposition incorporating clay and polyelectrolyte layers.[32] However, on the basis of morphology

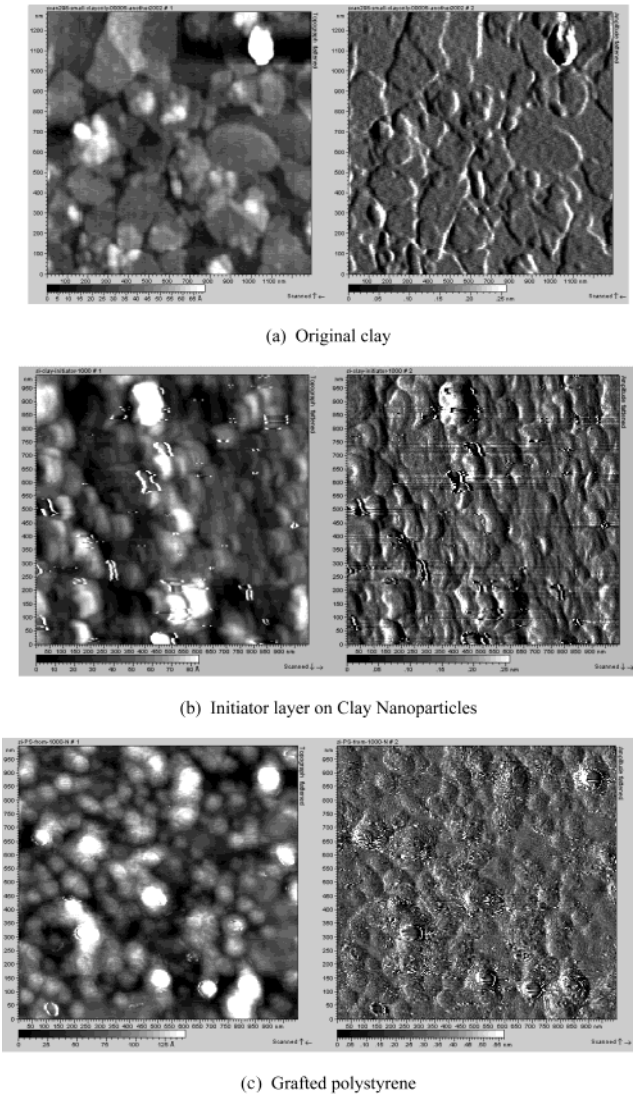

(a) Original clay

(b) Initiator layer on Clay Nanoparticles

(c) Grafted polystyrene

Figure 8. AFM morphologies of (a) original clay, (b) initiator on adsorbed clay nanoparticle layers, and (c) polymer brush layers grafted from clay surfaces (left image, topograph; right image, amplitude).

alone, it is not possible to determine actual grafting density of the initiators on clay. This can be verified by a combined QCM, impedance analysis, electrochemical, and thickness measurements.[11,34] Furthermore, the actual grafting density and morphology of the initiators during polymerization (and in solution) may change due to desorption.

In Figure 8c, the grafted polymer layer showed a remarkably different surface morphology (glassy state), exhibiting spherical or globular domains wherein portions of the surface are less covered (not uniform). In contrast with that of clay surfaces, the amplitude image becomes fuzzy because of greater adhesion force between the tip and the "softer" polystyrene brush layer. Other than the morphological inhomogeneity shown by the image, quantitative roughness data were also obtained by AFM. RMS roughness of the clay layer was calculated to be 3.2 nm. It increased to 4.1 nm for the polymer layer, indicating that more surface roughness was introduced by SIP. These results are consistent with broadening of the SPS reflectivity curve indicating increased inhomogeneity of the polymer layers. In comparison with previously reported SIP on Si and Au surfaces, an RMS roughness less than 1 nm has been reported by Prucker et al.[24]and Bruening et al., where they characterized the polymer layers to be

(40) Note that the interface of the flat surface is composed of a high concentration of growing chain ends confined in a limited two-dimensional area (Wittmer, J.; et al. *Europhys. Lett.* **1996**, *33*, 397). A large difference in surface tension can prevent the flux of monomer (typically nonpolar) at surfaces creating a more heterogeneous interfacial polymerization mechanism. A basic assumption on the theoretical treatment by Wittmer was that many simultaneously growing (essentially living) chains compete for the small influx of monomers to the surface. In this case, the difference between polarities at the interface and the nonpolar solvent subphase may prevent a homogeneous monomer influx. In effect, the polymerization system becomes a self-limiting heterogeneous system preventing formation of inherently high MW brushes. Also, the presence of any free initiators in solution competes with the polymerization of monomers, leaving less monomers available for polymerization at the interface and hence lower MW brushes.

(41) (a) Milner, S. T. *Science* **1991**, *252*, 905. (b) Milner, S. T.; Witten, T. A.; Cates, M. E. *Macromolecules* **1988**, *21*, 2610.

"very smooth". Again, this is attributed to the difference in polymer grafting density and the effects of a more ionic and polar surface on the polymerization mechanism.

Conclusions

A polystyrene brush layer with a thickness of about 8 nm was prepared through solution free radical SIP from adsorbed clay nanoparticle on solid support substrates. Flat substrate surfaces were first modified by SAMs to facilitate the electrostatic adsorption of clay and SIP initiator layers. The integrity of the clay, initiator, and polymer brush layers was confirmed by XPS, IR, SPS, and ellipsometry. By showing a step-by-step thickness increase, both ellipsometry and SPS verified formation of distinct layers on the SIP protocol. As compared with polymer brushes grafted directly from flat Si and Au surfaces, the lower thickness and rougher surfaces can be ascribed to a lower density of the active initiator sites on the clay surfaces. GPC analysis of the free polymers (from solution) and thickness measurements indicated a SIP saturation limit on the growth of polymer layer thickness. The effect of a more heterogeneous initiator surface (more polar or ionic) as compared to previously reported SIP protocols should be taken into account. Further kinetics studies and nanocomposite materials synthesis will be undertaken using the same methods.

Acknowledgment. This project was supported by the Army Research Office (Grant No. DAAD-19-99-1-0106). Montmorillonite clay was generously provided by Southern Clay Products, Inc. We appreciate Dr. Juan Pablo Claude and John Kestell at University of Alabama at Birmingham for IR analysis. We also acknowledge Dr. Earl Ada at the University of Alabama−Tuscaloosa for XPS measurements. Technical support from Optrel, GmBH is also acknowledged.

LA026039U